ORIGINAL RESEARCH

Ecology and Evolution   WILEY

Different processes shape the patterns of divergence in the nuclear and chloroplast genomes of a relict tree species in East Asia

Xiang-Yu Tian[1] (iD) | Jun-Wei Ye[2] | Tian-Ming Wang[1] | Lei Bao[1] | Hong-Fang Wang[1]

[1]State Key Laboratory of Earth Surface Processes and Resource Ecology and Ministry of Education Key Laboratory for Biodiversity Science and Ecological Engineering, College of Life Sciences, Beijing Normal University, Beijing, China

[2]Germplasm Bank of Wild Species in Southwest China, Kunming Institute of Botany, Chinese Academy of Sciences, Kunming, China

Correspondence
Hong-Fang Wang, State Key Laboratory of Earth Surface Processes and Resource Ecology and Ministry of Education Key Laboratory for Biodiversity Science and Ecological Engineering, College of Life Sciences, Beijing Normal University, Beijing 100875, China.
Email: wanghf@bnu.edu.cn

Abstract

Isolation by spatial distance (IBD), environment (IBE), and historical climatic instability (IBI) are three common processes assessed in phylogeographic and/or landscape genetic studies. However, the relative contributions of these three processes with respect to spatial genetic patterns have seldom been compared. Moreover, whether the relative contribution differs in different regions or when assessed using different genetic markers has rarely been reported. *Lindera obtusiloba* has been found to have two sister genetic clades of chloroplast (cpDNA) and nuclear microsatellite (nSSR), both of which show discontinuous distribution in northern and southern East Asia. In this study, we used the Mantel test and multiple matrix regression with randomization (MMRR) to determine the relative contributions of IBD, IBE, and IBI with respect to *L. obtusiloba* populations. Independent Mantel tests and MMRR calculations were conducted for two genetic data sets (cpDNA and nSSR) and for different regions (the overall species range, and northern and southern subregions of the range). We found a significant IBI pattern in nSSR divergence for all assessed regions, whereas no clear IBI pattern was detected with respect to cpDNA. In contrast, significant (or marginal) divergent IBD patterns were detected for cpDNA in all regions, whereas although a significant IBE was apparent with respect to the overall range, the effect was not detected in the two subregions. The differences identified in nSSR and cpDNA population divergence may be related to differences in the heredity and ploidy of the markers. Compared with the southern region, the northern region showed less significant correlation patterns, which may be related to the shorter population history and restricted population range. The findings of this study serve to illustrate that comparing between markers or regions can contribute to gaining a better understanding the population histories of different genomes or within different regions of a species' range.

KEYWORDS
East Asia, genetic marker, isolation by distance, isolation by environment, isolation by instability, regional history

1 | BACKGROUND

Disentangling the various contributions of geographical, environmental, and historical climatic dynamics to population genetic structures could provide significant insights into the species diversification (Lee & Mitchell-olds, 2011; Meirmans, 2012; Wang & Bradburd, 2014; Wright, 1943). Under the isolation-by-distance (IBD) scenario, gene flow is considered to be negatively correlated with geographical distance, and accordingly genetic differentiation between populations is expected to be positively correlated with distance (Hedrick, 2005; Meirmans, 2012; Wright, 1943). In contrast, the isolation-by-environment (IBE) hypothesis proposed that it is differences in environmental variables between sites that can explain most of the observed variance in gene flow and implies that local adaptation may occur and restrict the gene flow between sites (Manthey & Moyle, 2015; Sexton, Hangartner, & Hoffmann, 2014; Wang & Bradburd, 2014). In addition to IBD and IBE, historical climatic fluctuations, particularly glacial–interglacial cycles during the Pleistocene era (2.58–0.0117 million years ago, hereafter, Ma), have markedly influenced species distribution and demographic history (Qiu, Fu, & Comes, 2011; Soltis, Morris, McLachlan, Manos, & Soltis, 2006). These fluctuations in species distribution may subsequently lead to an instability in habitat connectivity and thereby contribute to enhancing population genetic differentiation. Isolation by instability (IBI) denotes a negative correlation between the extent of the historical instability of habitat connectivity and gene flow. Although both IBE and IBI can be calculated based on environment data, these processes differ in important respects, with IBE being characterized by the influence of differences in habitat environment on gene flow, whereas IBI is characterized by the influence of long-term habitat instability due to climate change and its resistance on dispersal between habitats. Previously, a number of studies have compared IBD and IBE to evaluate the contribution of local adaptation to present-day patterns in spatial genetic (Pelletier & Carstens, 2018; Sexton et al., 2014; Shafer & Wolf, 2013; Wang, Glor, & Losos, 2013). However, although the effect of historical climatic fluctuations on genetic diversity has been frequently described in phylogeographic studies, IBI has seldom been examined and compared with IBD and IBE [for rare examples, see _Lerista lineopunctulata_ Duméril & Bibron, 1839 (Sexton et al., 2014), _Quercus lobata_ Née (Gugger, Ikegami, & Sork, 2013) _Hypsiboas lundii_ Burmeister, 1856 (Vasconcellos et al., 2019)].

Owing to its extensive physiographical heterogeneity, in conjunction with frequent historical changes in climate and sea level, East Asia currently harbors the world's highest diversity of temperate flora (Qian & Ricklefs, 2000). It has been suggested that Cenozoic (66–23 Ma) relict genera in East Asia can be subdivided into two refugial regions (Milne & Abbott, 2002), namely the northern refugial region (NEA), comprising Japan, Korea, and adjacent areas of Northeast China, and the southern region (SEA), comprising south and southeastern China with extensions into Himalayan areas. These two refugial regions are divided by a low-precipitation zone, referred to as the "aridity belt" (Figure 1), which developed during the Eocene (56–33.9 Ma) and has persisted to the present day (Chen, Deng, Zhou, & Sun, 2018; Donoghue, Bell, & Li, 2001; Milne & Abbott, 2002). The arid belt is believed to represent a climatic barrier that restricts gene flow between the NEA and SEA regions (Bai, Wang, & Zhang, 2016; Milne & Abbott, 2002; Ye et al., 2017). Although studies over the past two decades have begun to focus on the spatial genetic patterns of temperate plant species in both the NEA and SEA regions and their responses to historical climate change (Chen et al., 2018; Harrison, Yu, Takahara, & Prentice, 2001; Qiu et al., 2011; Tang et al., 2018), the relative roles of spatial arrangement (IBD), local adaptation (IBE), and historical climate fluctuations (IBI) in shaping spatial genetic patterns in East Asia have rarely been thoroughly examined (but see He, Wang, Li, & Yi, 2016; Zhang, Wang, Comes, Peng, & Qiu, 2016).

Multiple factors can potentially influence the relative roles of IBD, IBE, and IBI in shaping spatial genetic patterns, including the genetic markers, regions, or species examined. Phylogeographic studies traditionally use chloroplast and nuclear markers, which have differing modes of inheritance, mutation rate, ploidy, and effective population size. Hence, independent spatial genetic patterns can be characterized for the two sets of markers under the same species demographic history and have frequently been reported in phylogeographic studies [e.g., _Vriesea gigantea_ Gaudich. (Palma-Silva et al., 2009), _Arabidopsis halleri_ (L.) O'Kane & Al-Shehbaz (Pauwels et al., 2012), _Juglans mandshurica_ Maxim. (Bai, Liao, & Zhang, 2010)]. Nonetheless, the examination of IBD-, IBE-, and IBI-related patterns in nuclear markers tends to be considerably more frequent than that using chloroplast markers. We assume that this disparity in usage can be attributed to the fact that IBD, IBE, and IBI have been studied to a greater extent in landscape genetics (in which chloroplast markers tend to be assessed less frequently) than in phylogeographic (Manel, Schwartz, Luikart, & Taberlet, 2003), which reflects the slight difference between the two fields (Rissler, 2016; Wang, 2010). Despite the disparate status of these markers, we maintain that comparisons among IBD, IBE, and IBI patterns based on both markers types would be necessary for gaining a more comprehensive understanding of the processes occurring in different genomes in the same cell, which in turn can contribute disentangling the complex processes associated with the origins of biodiversity.

As its designation indicates, the SEA is located in a lower latitude region than the NEA, and is also characterized by a higher degree of physiographical heterogeneity. Both pollen records and genetic data indicate that the SEA region has had the potential to sustain more refugia for temperate flora than the NEA region during glacial periods (Qian & Ricklefs, 2004; Qiu et al., 2011). Hence, we presume that IBD, IBE, and IBI processes would have differed to certain extents in the NEA and SEA regions. Although some independent studies have examined these processes in the SEA or entire region (He et al., 2016; Zhang et al., 2016), the regional differences between the NEA and SEA regions have yet to be compared. Moreover, even within the same region, different species with differing traits may show contrasting responses to IBD, IBE, and IBI. Accordingly, from the perspective of assessing the relative roles of these different
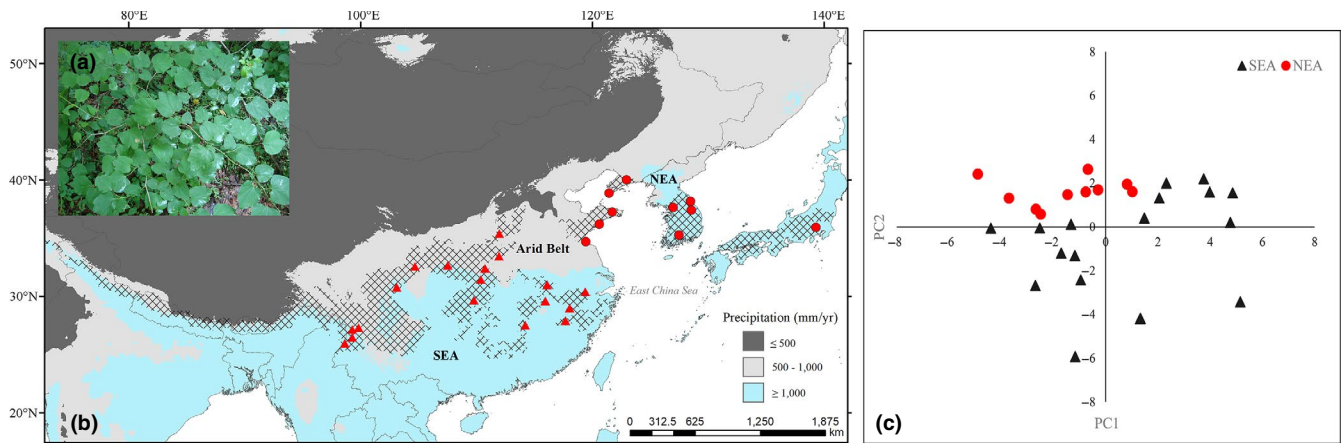
FIGURE 1 (a) An individual plant of *Lindera obtusiloba* showing the typical trilobed leaves. (b) The species range of *L. obtusiloba* (hatched area) and locations of the populations sampled in this study. The two sister genetic clades reported in a previous study (Ye et al., 2017) are denoted by different symbols: NEA clades, red circle; SEA clades, red triangle. The different colored areas of the map indicate the distribution of annual precipitation. This indicates that the approximate range of the two Cenozoic relict flora refugial regions in East Asia (NEA and SEA) is characterized by annual precipitation greater than 1,000 mm (Milne & Abbott, 2002). The region of low precipitation dividing the NEA and SEA (precipitation <1,000 mm) is referred to as the "arid belt," which is suggested to constitute a climatic barrier for species migration between the NEA and SEA regions (Milne & Abbott, 2002). (c) The PCA results for all sampled populations, indicating bioclimatic differences between populations. The black triangles and red circles represent SEA and NEA clade populations, respectively

processes, studies of widespread species with sister clades in the NEA and SEA regions would contribute to minimizing species difference and maximizing regional differences.

Lindera obtusiloba Blume is a drought-sensitive deciduous shrub or small tree that has a widespread distribution in both the NEA and SEA regions (Figure 1). In a previous study on this species (Ye et al., 2017), both chloroplast DNA sequence (cpDNA) and nuclear microsatellite (nSSR) data indicated the occurrence of two clearly discontinuous genetic clades in the NEA and SEA regions (Figure 1). Over the entire distribution range of *L. obtusiloba*, the greatest divergence in the populations of this species occurs between the NEA and SEA populations. Both the most recent common ancestor of cpDNA haplotypes and population divergence estimates based on nSSRs have dated the divergence between NEA and SEA populations to the Pliocene (5.33–2.58 Ma; Ye et al., 2017). Notable in this regard is the fact that the genetic break between NEA and SEA populations of *L. obtusiloba* is considerably sharper than that reported for other species with a similar distribution, for example, Asian butternuts (Bai et al., 2016), *Acer mono* Maxim. (Guo et al., 2014), *Kalopanax septemlobus* Koidz. (Sakaguchi et al., 2012), and *Prinsepia* Royle (Ma, Wang, Tian, & Sun, 2019). We suspect that this abrupt genetic break between *L. obtusiloba* populations could be attributed to the drought sensitivity of the species and that the arid belt located between NEA and SEA regions may represent a strong climatic barrier to the spread of *L. obtusiloba*.

The findings of both field and common garden studies have indicated that the NEA and SEA populations of *L. obtusiloba* can be distinguished with respect to seed weight and multiple phenological traits, including bud break and fruit maturation (Dai, 2019). In spite of such trait differences, however, the two genetic clades are sister clades that are characterized by similar climatic niches (Tian 2019, unpublished data). Hence, *L. obtusiloba* would appear to provide an

ideal system for comparative analysis of evolutionary processes occurring in the NEA and SEA regions. In this regard, although Ye et al. (2017) have previously provided a detailed description of the spatial genetic patterns of *L. obtusiloba* in the NEA and SEA regions, there has to date been no comparative examination of the relative contributions of IBD, IBE, and IBI to present-day distributions. Moreover, Ye et al. (2017) found that compared with SEA populations of *L. obtusiloba*, those in the NEA harbors a higher genetic diversity of nSSRs, although not of cpDNA, thereby implying the differential history of the two marker types. Accordingly, on the basis of a combination of cpDNA and nSSR data and ecological niche modeling (ENM), we examined IBD, IBE, and IBI patterns in both types of markers with respect to the overall range of *L. obtusiloba* and also that in the two divided subregions (NEA and SEA). Our goal was to identify potential differences in the evolutionary processes occurring in the different regions and for different types of genetic markers.

2 | METHODS

2.1 | Genetic differentiation

In the present study, we used a data set previously compiled by Ye et al. (2017), which comprises the genotypic data of six nSSRs for 659 individuals and those of four cpDNA fragments (*psbA–trnH*, *trnL–trnF*, *trnS–trnG*, and *rpl16*) for 271 individuals. The individuals analyzed were derived from 28 populations (10 in the NEA and 18 in the SEA; Figure 1; Appendix S1). The sampled populations were scattered across an area representing the major distribution of the species. More than three voucher specimens of each sampled population have been archived in the herbarium of Beijing Normal University. The cpDNA data have been deposited in GenBank with

the accession nos. KU645591–KU645758. Multiple population genetic distance indices were determined for both nSSRs and cpDNA, which constitute a comprehensive map of population genetic divergence (Appendix S2). For cpDNA, we calculated the population genetic distance indices N_{ST}, G_{ST}, and D_{xy} using DnaSP version 6.12.03 (Rozas et al., 2017), and for nSSRs, the population genetic distance indices F_{ST} and R_{ST} were calculated using GenAlEx 6.5 (Peakall & Smouse, 2012) and SPAGeDi 1.5 (Hardy & Vekemans, 2002), respectively. All calculations for genetic distance indices were performed using the default settings in each program.

2.2 | Geographical distance

We represented the locations of the sampled populations in terms of longitude and latitude under the Beijing 1954 projection system. Pairwise geographical distances between sampled populations were calculated by using the function "distm" in the package "geosphere" (Hijmans, 2015) of R version 3.6.0 (R Development Core Team, 2013). For distance computation, we applied the "distVincentyEllipsoid" function, which calculates the shortest circle distance between points.

2.3 | Environmental distance

As environmental variables, we used the data of 19 bioclimatic variables for the current period (1950–2000) obtained from the WorldClim database (Fick & Hijmans, 2017; Hijmans, Cameron, Parra, Jones, & Jarvis, 2005; Appendix S3). All climate layers used in this study were prepared at a resolution of 2.5 arc minutes. For each of the 28 sampling sites, the 19 bioclimatic variables were extracted using ArcGIS 10.1 (ESRI). To characterize major environmental variation, we performed principal component analysis (PCA) using the "prcomp" function in R version 3.6.0 (R Development Core Team, 2013). Given that the first two coordinates of PCA (PC1 and PC2) can account for most of the environmental variability, we calculated the environmental distances between each of the sampled populations on the first two PC axes using the "vegdist" function based on the Euclidean method in the "vegan" package (Oksanen, Blanchet, Kindt, Legendre, & Minchin, 2017) of R version 3.6.0.

2.4 | Resistance distance

To assess the influence of the historical instability of habitat connectivity on population genetic differentiation, we modeled the distributions of suitable habitats for the present, last glacial maximum (LGM; 21 thousand years ago, hereafter, kya), and last interglacial (LIG; 120 kya) periods based on ecological niche modeling (ENM) in MAXENT (Phillips & Dudík, 2008). The ENM procedure and the results obtained using this procedure have been described in detail in our previous study (Ye et al., 2017). In brief, 100 occurrence sites

of *L. obtusiloba* showing no spatial redundancy were included in the ENM. The locations of these 100 sites and data sources can be found in Appendix S4. The modeling included only 11 bioclimatic variables that lacked strong correlation (*r* < .9), namely annual mean temperature, mean diurnal range, isothermality, temperature seasonality, maximum temperature of the warmest month, minimum temperature of the coldest month, mean temperature of the wettest quarter, annual precipitation, precipitation of the wettest month, precipitation of the driest month, and precipitation seasonality. Model validation was performed via 10 independent runs with 20% randomly selected data. High receiver operating characteristic (ROC) values (0.928 ± 0.025) have been reported for this type of modeling, which indicate its good accuracy. The established model was projected onto LGM (MIROC-ESM) and LIG climatic models (Shields et al., 2012; Watanabe et al., 2011).

The climatic suitability of each grid in each period was described in terms of the species occurrence possibility obtained from the ENM results for *L. obtusiloba*. To calculate resistance distance, the climatic suitability of each period was converted into a resistance value as climatic unsuitability ("1-suitability"), using the "create friction layer" function in the SDM toolbox (Brown, 2014; Brown, Bennett, & French, 2017). The historical climate instability resistance map was represented by the overall climate unsuitability from LIG to the present, calculated by adding the unsuitability values of each period. The values of the resistance map ranged from 0 to 3, with 0 representing the lowest climate instability resistance due to highest habitat suitability in each period and 3 representing the highest climate instability resistance due to lowest habitat suitability in each period (Figure 2).

On the basis of the historical climate instability resistance map, we calculated resistance distance among 28 populations according to circuit theory in Circuitscape v4.0 (McRae, Dickson, Keitt, & Shah, 2008; Shah & McRae, 2008).

2.5 | IBD, IBE, and IBI analyses

To investigate the relationships between ecological factors (geographical, environmental, and historical habitat instability) and population genetic differentiation, we performed Mantel tests with 10,000 permutations for each genetic distance index of both marker types (nSSRs: F_{ST} and R_{ST}; cpDNA: N_{ST}, G_{ST}, and D_{xy}). To disentangle the potentially complex interactions among geographical distance, environmental distance, and resistance distance and compare the relative contribution of IBD, IBE, and IBI on population differentiation, we used multiple matrix regression with randomization (MMRR) based on 10,000 permutations. All variables included in the aforementioned analyses were standardized using the "scale" function in the "vegan" package (Oksanen et al., 2017). Both the Mantel test and MMRR analysis were performed using the R program (R Development Core Team, 2013).

To compare the processes shaping the spatial genetic structure in the NEA and SEA regions, we performed the same Mantel test

and MMRR analyses using only data pertaining to the NEA or SEA, respectively.

When performing analyses, we did not take into consideration nonlinear relationships. Although certain variables probably showed nonlinear relationships with genetic distance, their linear relationships were still significant in this study. Moreover, whereas a linear fit may not the best fit for these relationships, from the perspective of simplification, we only included linear relationships for variables when comparing the relative contributions of IBD, IBE, and IBI to spatial genetic patterns. Therefore, the use of a linear model may represent a more conservative test of the relationships.

3 | RESULTS

3.1 | Environmental analyses

The results of PCA indicated that the first two coordinates (PC1 and PC2) accounted for 67.24% of the environmental variation. For PC1, environmental variables related to humidity (e.g., annual precipitation, precipitation of the wettest quarter, precipitation of the driest quarter, and precipitation of the coldest quarter) had the highest weights, whereas for PC2, temperature-related variables (e.g., isothermality, temperature seasonality, maximum temperature of the warmest month, and temperature annual range) had the highest weights (Appendix S3). Neither PC1 nor PC2 values showed significant differences between the NEA and SEA regions, whereas the points pertaining to the NEA populations were clustered when combined PC1 and PC2, implying that habitat in the NEA was probably a marginal type of that in the SEA (Figure 1c).

ENM results (Ye et al., 2017) indicated that the area of habitats in the SEA with suitable climates was larger during the LGM than the present-day distributions, whereas the area in the NEA was more climatically limited. Furthermore, during the LIG, the area of suitable habitats in both NEA and SEA regions was smaller than that during the present and LGM periods.

Climate instability resistance values, which were obtained based converting the ENM results and summing over the three periods, showed an uneven spatial distribution (Figure 2). We found that the central SEA region and the Japanese Archipelago in the NEA had larger continuous ranges of long-term stable habitats than the remaining areas of species' range, which indicates a lower climate instability resistance for long-term gene flow in these two regions. Interestingly, the population genetic differentiation of nSSRs was found to be generally lower in the central SEA region and Japanese Archipelago (Figure 2a), whereas no comparable pattern was observed with respect to cpDNA (Figure 2b).

3.2 | IBD, IBE, and IBI in nSSRs

nSSR analysis indicated that in both the NEA and SEA regions, F_{ST} and R_{ST} showed significantly positive relationships with

geographical distance (F_{ST}: $r = .5221$, $p = .0001$; R_{ST}: $r = .5469$, $p = .0001$) and climatic instability resistance (F_{ST}: $r = .5781$, $p = .0001$; R_{ST}: $r = .5505$, $p = .0001$) based on the Mantel test (Figure 3; Appendix S5). MMRR analysis indicated that climatic instability resistance (F_{ST}: $\beta = 0.1230$, $p = .0001$; R_{ST}: $\beta = 0.1308$, $p = .0001$) can explain more variance in F_{ST} or R_{ST} than geographical distance (F_{ST}: $\beta = 0.0577$, $p = .0103$; R_{ST}: $\beta = 0.1035$, $p = .0003$; Table 1), thereby indicating a stronger IBI pattern than that of IBD. In the MMRR analysis (Table 1), F_{ST} showed a significant negative relationship with environmental distance ($\beta = -0.0468$, $p = .0024$), whereas the Mantel test indicated that R_{ST} has a significantly positive relationship with environmental distance ($r = .2106$, $p = .0012$). This seemingly contradictory pattern may indicate a weak effect of IBE over the entire species range.

Both the Mantel test and MMRR analysis indicated a significantly positive relationship between climatic instability resistance and F_{ST}/R_{ST} (Mantel: F_{ST}: $r = .3279$, $p = .0064$; R_{ST}: $r = .4237$, $p = .0004$; MMRR: F_{ST}: $\beta = 0.1153$, $p = .0393$; R_{ST}: $\beta = 0.2226$, $p = .0017$; Table 1; Appendix S7), which is indicative of a strong IBI pattern. Geographical distance showed a significantly positive relationship with R_{ST} based on the Mantel test, whereas we were unable to detect any significant relationships when performing MMRR analysis. In contrast, environmental distance showed a significant negative relationship with both F_{ST} ($\beta = -0.0443$, $p = .0402$) and R_{ST} ($\beta = -0.0844$, $p = .0227$) based on the MMRR analysis, whereas significant relationships were detected using the Mantel test. The contrasting patterns for geographical and environmental distances identified using the Mantel test and MMRR analysis may indicate the weak effects of these two factors on the nuclear genetic patterns in the SEA region.

For the NEA region, the weak IBI pattern we identified may be attributable to the fact that only R_{ST} showed a relatively consistent IBI pattern. Although the Mantel test did not identify significant relationships for R_{ST}, with respect to geographical and environmental distances, it indicates a marginally significant positive relationship with climatic instability resistance ($r = .2657$; $p = .0784$; Appendix S8), whereas MMRR analysis identified a positive relationship with climatic instability resistance ($\beta = 0.2067$; $p = .0071$) and a negative relationship with geographical distance ($\beta = -0.0794$; $p = .0021$; Table 1). With respect to F_{ST}, the Mantel test indicated a significant positive relationship with both geographical distance ($r = .5920$, $p = .0135$) and climatic instability resistance ($r = .5817$, $p = .0003$), whereas MMRR analysis failed to identify any significant relationships for the three distance indices. Thus, on the basis of the present analyses, we were unable to identify any clear patterns in IBD or IBE in the NEA region.

3.3 | IBD, IBE, and IBI in cpDNA

Our analyses of the chloroplast genome revealed differences in the correlation patterns of the three genetic distance indices throughout the entire distribution range of *L. obtusiloba*. Using the
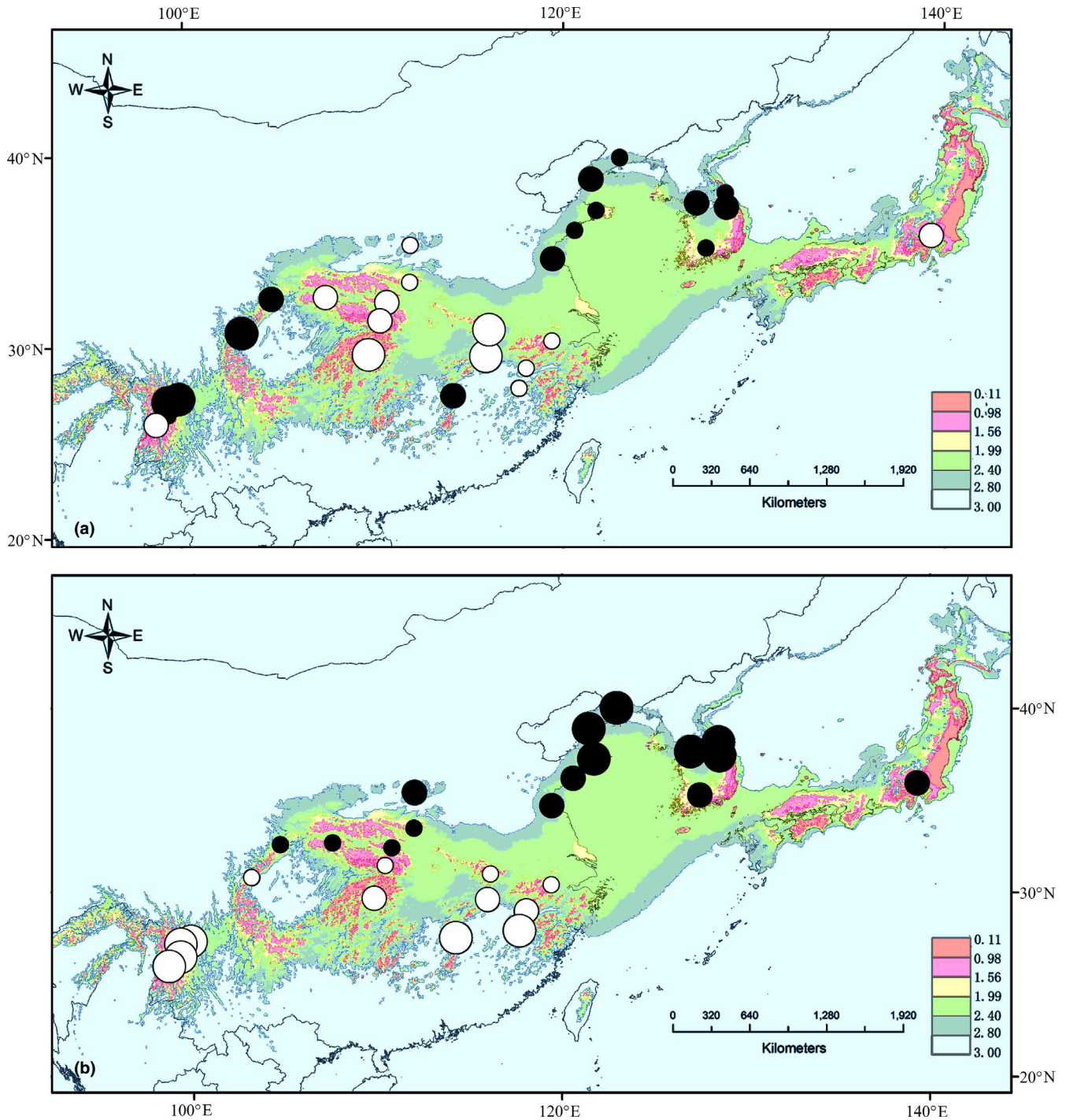
FIGURE 2 The geographical distribution of population genetic distances for (a) the nSSR index R_{ST} and (b) the cpDNA index D_{XY}. The population genetic distance of each sampled populations is represented by the average R_{ST} (or D_{XY}) with that of each of the other populations. A higher than the species-level average R_{ST} (or D_{XY}) value is represented by a black circle, whereas a lower than average value is denoted by a while circle. The size of the circles is proportional to the difference from the average value. The background map in both (a) and (b) is the historical climatic instability resistance map, with 0 representing the lowest climate instability resistance due to the highest habitat suitability in each period [last interglacial (LIG), last glacial maximum (LGM), and the present), and 3 representing the highest climate instability resistance due to the lowest habitat suitability in each period

Mantel test, we found that genetic distance D_{xy}, which indicates divergence since the last common ancestor between populations, was significantly correlated with the three factors (Figure 4), with

the highest correlation value observed for geographical distance (r = .4108, p = .0001). MMRR analysis revealed that D_{xy} was only influenced by geographical distance (β = 0.0006, p = .0007; Table 1).
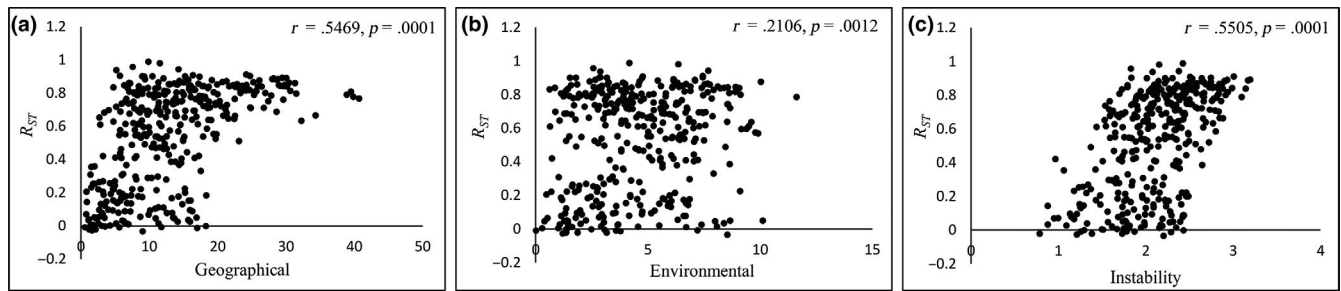
FIGURE 3 Scatter plots showing the relationships between the population genetic distance index R_{ST} (nSSR) and (a) geographical distance, (b) environmental distance, and (c) climatic instability resistance distance. The statistical results of Mantel tests are shown in the upper right-hand corner of each plot

Genetic distance N_{ST} takes into account both the allele frequency between populations and allele genetic distance, and was found to be significantly correlated with the three factors in the Mantel test, with the highest correlation value ($r = .3607$, $p = .0001$) being identified for environmental distance (Appendix S6), whereas N_{ST} was only influenced by environmental distance based on the MMRR analysis ($\beta = 0.0791$, $r = .0008$; Table 1). The disparity between the results obtained using the Mantel test and MMRR analysis may be attributable to the collinearity between geographical distance and climatic instability resistance ($\beta = 0.758$, $p = .000$). In this regard, we suspect that the results of MMRR analysis may be more accurate than those obtained the Mantel test, as MMRR simultaneously considers all factors. For G_{ST}, which only applies to the allele frequency between populations, both the Mantel test and MMRR analysis showed significantly positive correlation with environmental distance (Mantel test: $r = .2025$, $p = .0381$; MMRR analysis: $\beta = 0.0932$, $r = .0146$; Table 1; Appendix S6). G_{ST} appeared to show no clear IBD pattern, given that the Mantel test revealed

no significant correlations and MMRR analysis revealed an anomalously significant negative relationship.

For the SEA region, we found that the distribution of D_{xy} shows a pattern similar to that observed for the entire species range, with a significant IBD pattern (Mantel test: $r = .5459$, $p = .0001$; MMRR analysis: $\beta = 0.0010$, $p = .0003$) but no clear IBE or IBI patterns (Appendix S7). Although MMRR analysis indicated that neither N_{ST} nor G_{ST} showed significant IBD, IBE, or IBI patterns (Table 1), the Mantel test indicated that N_{ST} showed a significantly positive correlation with all three factors when tested independently (IBD, $r = .3752$, $p = .0001$; IBE, $r = .3344$, $p = .0002$; IBI, $r = .3690$, $p = .0027$; Appendix S7).

With the exception of a marginally significant positive correlation between D_{xy} and geographical distance (Mantel test: $r = .4112$, $p = .0670$; MMRR analysis: $\beta = 0.0002$, $p = .0926$), we were unable to detect any significant IBD, IBE, or IBI patterns with respect to genetic distance indices in the NEA region (Table 1; Appendix S8).

TABLE 1 Multiple matrix regression with randomization (MMRR) analysis results showing the relative contribution of isolation by spatial distance (IBD), environment (IBE), and historical climatic instability (IBI) with respect to multiple population genetic distance indices of both nSSRs and cpDNA markers in the overall range (overall) of *Lindera obtusiloba* and two subregions (NEA and SEA) within this range

| Regions	Genetic divergence	β_{Total}	β_{IBD}	β_{IBE}	β_{IBI}
Overall nSSRs	F_{ST}	0.6227**	0.0577*	−0.0468**	0.123**
	R_{ST}	0.5898**	0.1035**	−0.0261	0.1308**
Overall cpDNA	G_{ST}	0.4056*	−0.1445*	0.0932*	0.0924
	N_{ST}	0.3746**	0.0169	0.0791**	0.0178
	D_{xy}	0.4211**	0.0006**	−0.0001	0.0002
NEA nSSRs	F_{ST}	0.6503*	0.0229	−0.0002	0.0525
	R_{ST}	0.6101*	−0.0794**	−0.0065	0.2067**
NEA cpDNA	G_{ST}	0.454	−0.1195	0.0316	0.2689
	N_{ST}	0.4534	−0.1369	0.0344	0.3404
	D_{xy}	0.4464	0.0002	−0.0001	0.0000
SEA nSSRs	F_{ST}	0.4064*	−0.0118	−0.0443*	0.1153*
	R_{ST}	0.4710**	0.0126	−0.0844*	0.2226**
SEA cpDNA	G_{ST}	0.3587	−0.1422	0.0393	0.1706
	N_{ST}	0.4062*	0.0411	0.0282	0.0546
	D_{xy}	0.5961**	0.0010**	−0.0001	−0.0005

*.01 < p < .05;

**p < .01.
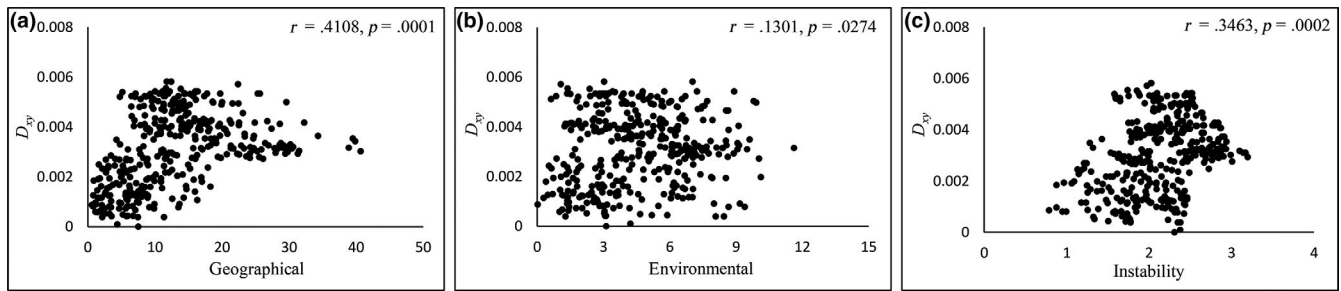
FIGURE 4 Scatter plots showing the relationships between the population genetic distance index D_{XY} (cpDNA) and (a) geographical distance, (b) environmental distance, and (c) climatic instability resistance distance. The statistical results of Mantel tests are shown in the upper right-hand corner of each plot

4 | DISCUSSION

4.1 | Different processes underlying genetic differentiation in the nuclear and chloroplast genome

In this study, we identified differences in the processes underlying the divergent genetic patterns in nSSRs and cpDNA in *L. obtusiloba*. With respect to nSSRs, we detected significant IBI and IBD patterns over the entire species range, with the contribution of IBI being found to be greater than that of IBD. Given that neither of the NEA and SEA subregions show a clear IBD pattern, we infer that the observed IBD pattern over the entire range may have been primarily influenced by the greatest population divergence between the NEA and SEA regions, which has been reported previously by Ye et al. (2017). Thus, climatic instability since the late Pleistocene is likely to have been the main driving force underlying the nuclear genetic patterns observed in *L. obtusiloba*.

Our observations indicate that climate instability resistance between populations would not appear to explain the genetic divergence of cpDNA. However, the genetic distance index D_{xy} shows a clear IBD pattern, and the genetic differentiation of the indices N_{ST} and G_{ST} shows a clear IBE pattern over the entire range of the species. We suspect that local adaptation to different environments in the NEA and SEA regions (Figure 2) may have driven chloroplast divergence in the population. Generally, the NEA region is considered to have greater seasonality than the SEA region with respect to temperature and precipitation (Bai et al., 2016; Qiu et al., 2011). Although we were unable to detect any significant differences between the habitats of *L. obtusiloba* in NEA and SEA regions in relation to humidity (PC1) nor heat (PC2), the habitat types in the NEA are unique when these two climatic factors are considered together. We suspect that habitat in the NEA region is a marginal type of that in the SEA region (Figure 1c; Appendix S4). Local adaptation in marginal habitats has been reported in several species, including *Arabidopsis lyrata* (Linnaeus) O'Kane & Al-Shehbaz (Hämälä, Mattila, & Savolainen, 2018), *Ambrosia artemisiifolia* L. (van Boheemen, Atwater, & Hodgins, 2019), and *Mimulus guttatus* DC. (Ferris, Barnett, Blackman, & Willis, 2017). In addition, population divergence of *L. obtusiloba* in the two regions is estimated to have undergone divergence in the Pliocene and gene flow between the

two regions is rare (Ye et al., 2017). Hence, local adaptations may have evolved in the two regions, and indeed, differences of multiple functional traits between populations in the NEA and SEA regions, including fruit morphology and the phenology of bud break and fruit maturation, have been observed in either field or common garden studies (Dai, 2019). Compared with IBD or IBI, the IBE patterns detected in the genome can be heterogeneous, as these patterns tend to be driven primarily by selection against immigration (Sexton et al., 2014; Wang & Bradburd, 2014). Therefore, analysis of a limited number of nSSR loci may not be sufficient to detect a significant IBE pattern in the nuclear genome.

The heredity of nuclear and chloroplast genomes may have contributed to the contrasting responses of these genomes to historical climate instability. The chloroplasts in our study species are maternally inherited and can only be transmitted to offspring by seed flow, whereas the nuclear genomes are biparentally inherited and can be transmitted via both seed and pollen flows. Dispersal of the seeds and pollen of *L. obtusiloba* is mediated by birds and insects, respectively (Smith, Hamel, Devall, & Nathan, 2004), and previous phylogeographic studies and fossils data indicate that climate change can affect the distribution of these vector species (Dong et al., 2017; Kharouba, Lewthwaite, Guralnick, Kerr, & Vellend, 2019; Wang, Zhu, Heller, Zhou, & Shi, 2020). Hence, it is to be assumed that dispersal based on these species would be influenced to a considerable extent by climate fluctuations (Guisan & Thuiller, 2005; Pearson & Dawson, 2003; Van der Putten, Macel, & Visser, 2010). Moreover, compared with birds, insects typically have a limited range of dispersal (Phillipsen et al., 2015; Phillipsen & Lytle, 2013). Accordingly, given that patterns in the nuclear genome can reflect the dispersal patterns of both seed and pollen, the effect of climate instability on bird and insect distribution may have resulted in a stronger IBI pattern in the nuclear genome compared with that of the chloroplast.

In addition to the contrasting modes of heredity, differences in ploidy may also have contributed to the different correlation patterns we detected for the two genomes. The nuclear genome is diploid, undergoes recombination, and generally has a larger effective population size than the chloroplast, which is haploid and does not recombine (Gaudeul, Gardner, Thomas, Ennos, & Hollingsworth, 2014; McCauley, 1994). Hence, the nuclear genome might be excepted to have a higher mutation rate and genetic diversity than the

chloroplast, which could reflect the greater effect the more substantial influence of recent historical climate change on the gene flow between populations (Bai et al., 2010). In addition, nSSRs, which are markers commonly used in phylogeographic studies, have a considerably higher mutation rate than cpDNA sequences, which may enhance the observed IBI pattern. In summary, differences in heredity and ploidy between the nuclear and chloroplast genomes or the differences between nSSR and cpDNA sequences could account for the stronger IBI pattern in nSSRs that we observed in the present study.

4.2 | Genetic patterns in the SEA region are more pronounced than those in the NEA region

Although we identified similarities in the correlation patterns detected for the NEA and SEA regions, we found the patterns in the SEA region to be considerably more significant than those in the NEA region. With respect to nSSRs, both F_{ST} and R_{ST} showed a significant IBI pattern in the SEA region, whereas only R_{ST} showed a significant IBI pattern in the NEA region. For cpDNA, whereas D_{xy} showed a significant IBD pattern in the SEA region, the pattern for this index was only marginally significant in the NEA region. We suspect that the stronger IBI and IBD patterns detected for SEA region could be related to a combination of topographical differences and Pleistocene climatic oscillations.

Populations of temperate plants in the NEA and SEA regions probably underwent different rates and extents of expansion and contractions in response to Pleistocene climate fluctuations (Milne & Abbott, 2002; Qiu et al., 2011). In the SEA region, both molecular and ENM evidence indicate that numerous locations in the western, central, and eastern mountainous areas may have served as glacial refugia for *L. obtsuloba* (Ye et al., 2017). The combination of climate instability and geological isolations would thus have led to a negative correlation between gene flow and resistance or geographical distance, thus resulting in significant IBI or IBD patterns.

Although molecular data for the NEA region indicate long-term persistence, most populations, particularly those on the mainland, were formed recently via postglacial migration from the southern margins of the NEA or Japanese Archipelago. Inferences with respect to NEA and SEA glacial refugia are also supported by the distribution of climatically stable habitats during the late Pleistocene (Figure 2). These findings indicate that most NEA populations have a more recent population history than those in the SEA region. In addition, the southern clades in the SEA region have a considerably wider distribution than clades in the NEA region. Although the number of populations we sampled in the NEA (10 populations) was smaller than the number examined in the SEA region (18 populations), we do not believe this to be a prominent factor accounting for the less pronounce genetic patterns detected in the NEA. Relative to their respective range sizes, sampling densities in the two regions were similar, and thus, the influence of sampling effort on characterizing spatial variance in the two regions would be comparable. Insufficient

time and/or space can restrict the effects of evolutionary forces (such as drift or selection) and thereby reduce the significance of detected patterns (Holderegger, Buehler, Gugerli, & Manel, 2010; Sexton et al., 2014). In the NEA region, the shorter evolutionary history and relatively homogeneous topographical have probably been important factors contributing to limited drift and geographical isolation. Moreover, postglacial expansion occurred in a restricted population range in the mainland area of the NEA region, which may also have contributed to limited population genetic divergence. Hence, the less prominent IBI or IBD patterns we identified in the NEA region may be related to the recent population history and restricted population range of *L. obtusiloba* in this region.

5 | CONCLUSIONS

In this study, we compared the relative contributions of IBD, IBE, and IBI to the genetic divergence of *L. obtusiloba* in East Asia, based on analyses of different types of genetic marker and different regions. We found that different processes have probably driven the patterns of nuclear and chloroplast genetic divergence. The divergence of nSSRs appears to have been influenced primarily by the historical climatic instability (IBI) over either the entire species range or within the two distinct subregions (NEA and SEA) of this range. In contrast, we were unable to detect any significant IBI pattern with respect to the divergence of cpDNA. We envisage that changes in climatic change during the late Pleistocene have had a stronger influence on population divergence of the nuclear genome than that of the chloroplast genome, which can probably be attributed to differences in the inheritance mode and ploidy of these two genomes. Differences in the patterns of cpDNA divergence are assumed to be influenced by spatial distribution (IBD). In addition, local adaptation may have affected the divergence of the chloroplast between the northern and southern regions, whereas we detected no clear IBE pattern for nuclear divergence based on the set of nuclear loci analyzed in the present study.

We also identified convergence in the correlation patterns of both the nuclear and chloroplast genomes in the NEA and SEA regions. However, due to the shorter population history and more restricted population range of *L. obtusiloba* in the NEA, we found this region to be characterized by a less significant pattern of genetic divergence than the SEA region. Collectively, the findings of this study serve to emphasize that even within a single species, analysis of different genetic markers or different regions can reveal differences in IBD, IBE, or IBI patterns or differing extent of significance. Such findings will contribute to gaining a more complete understanding of the population history of different genomes or patterns of divergence in different regions of a species' range.

DATA AVAILABILITY STATEMENT

The chloroplast DNA sequence data have been deposited in GenBank with accession nos. KU645591–KU645758. Data relating to MaxEnt files, and microsatellite genotypes have been uploaded to DRYAD: https://datadryad.org/stash/share/4ihCPpUOWD_zNdlbsTdxDwWD5uGcM7Qm0sI6LcW-5aE.

ORCID

Xiang-Yu Tian 🆔 https://orcid.org/0000-0002-2707-6908

REFERENCES

Bai, W. N., Liao, W. J., & Zhang, D. Y. (2010). Nuclear and chloroplast DNA phylogeography reveal two refuge areas with asymmetrical gene flow in a temperate walnut tree from East Asia. *New Phytologist*, *188*(3), 892–901. https://doi.org/10.1111/j.1469-8137.2010.03407.x

Bai, W. N., Wang, W. T., & Zhang, D. Y. (2016). Phylogeographic breaks within Asian butternuts indicate the existence of a phytogeographic divide in East Asia. *New Phytologist*, *209*(4), 1757–1772. https://doi.org/10.1111/nph.13711

Brown, J. L. (2014). SDMtoolbox: A python-based GIS toolkit for landscape genetic, biogeographic and species distribution model analyses. *Methods in Ecology and Evolution*, *5*(7), 694–700. https://doi.org/10.1111/2041-210X.12200

Brown, J. L., Bennett, J. R., & French, C. M. (2017). SDMtoolbox 2.0: The next generation Python-based GIS toolkit for landscape genetic, biogeographic and species distribution model analyses. *PeerJ*, *5*, e4095. https://doi.org/10.7717/peerj.4095

Chen, Y. S., Deng, T., Zhou, Z., & Sun, H. (2018). Is the East Asian flora ancient or not? *National Science Review*, *5*(6), 920–932.

Dai, M. J. (2019). *The evolution of the traits of* Lindera obtusiloba *– based on foeld and common garden*. Master, Beijing Normal University.

Dong, F., Hung, C. M., Li, X. L., Gao, J. Y., Zhang, Q., Wu, F., … Yang, X. J. (2017). Ice age unfrozen: Severe effect of the last interglacial, not glacial, climate change on East Asian avifauna. *BMC Evolutionary Biology*, *17*(1), 244. https://doi.org/10.1186/s12862-017-1100-2

Donoghue, M. J., Bell, C. D., & Li, J. (2001). Phylogenetic patterns in Northern Hemisphere plant geography. *International Journal of Plant Sciences*, *162*(S6), S41–S52. https://doi.org/10.1086/323278

Ferris, K. G., Barnett, L. L., Blackman, B. K., & Willis, J. H. (2017). The genetic architecture of local adaptation and reproductive isolation in sympatry within the *Mimulus guttatus* species complex. *Molecular Ecology*, *26*(1), 208–224. https://doi.org/10.1111/mec.13763

Fick, S. E., & Hijmans, R. J. (2017). WorldClim 2: New 1-km spatial resolution climate surfaces for global land areas. *International Journal of Climatology*, *37*(12), 4302–4315. https://doi.org/10.1002/joc.5086

Gaudeul, M., Gardner, M. F., Thomas, P., Ennos, R. A., & Hollingsworth, P. M. (2014). Evolutionary dynamics of emblematic Araucariaspecies (Araucariaceae) in New Caledonia: Nuclear and chloroplast markers suggest recent diversification, introgression, and a tight link between genetics and geography within species. *BMC Evolutionary Biology*, *14*(1), 171. https://doi.org/10.1186/s12862-014-0171-6

Gugger, P. F., Ikegami, M., & Sork, V. L. (2013). Influence of late Quaternary climate change on present patterns of genetic variation in valley oak, Quercus lobata Née. *Molecular Ecology*, *22*(13), 3598–3612. https://doi.org/10.1111/mec.12317

Guisan, A., & Thuiller, W. (2005). Predicting species distribution: Offering more than simple habitat models. *Ecology Letters*, *8*(9), 993–1009. https://doi.org/10.1111/j.1461-0248.2005.00792.x

Guo, X. D., Wang, H. F., Bao, L., Wang, T. M., Bai, W. N., Ye, J. W., & Ge, J. P. (2014). Evolutionary history of a widespread tree species *Acer mono* in East Asia. *Ecology and Evolution*, *4*(22), 4332–4345.

Hämälä, T., Mattila, T. M., & Savolainen, O. (2018). Local adaptation and ecological differentiation under selection, migration, and drift in *Arabidopsis lyrata**. *Evolution*, *72*(7), 1373–1386. https://doi.org/10.1111/evo.13502

Hardy, O. J., & Vekemans, X. (2002). spagedi: A versatile computer program to analyse spatial genetic structure at the individual or population levels. *Molecular Ecology Notes*, *2*(4), 618–620. https://doi.org/10.1046/j.1471-8286.2002.00305.x

Harrison, S. P., Yu, G., Takahara, H., & Prentice, I. C. (2001). Diversity of temperate plants in east Asia. *Nature*, *413*(6852), 129–130. https://doi.org/10.1038/35093166

He, S. L., Wang, Y. S., Li, D. Z., & Yi, T. S. (2016). Environmental and historical determinants of patterns of genetic differentiation in wild soybean (Glycine soja Sieb. et Zucc). *Scientific Reports*, *6*, 22795. https://doi.org/10.1038/srep22795

Hedrick, P. W. (2005). A standardized genetic differentiation measure. *Evolution*, *59*(8), 1633–1638. https://doi.org/10.1111/j.0014-3820.2005.tb01814.x

Hijmans, R. J. (2015). Geosphere: spherical trigonometry. R package version. 1.3-13. https://CRAN.Rproject.org/package=geosphere

Hijmans, R. J., Cameron, S. E., Parra, J. L., Jones, P. G., & Jarvis, A. (2005). Very high resolution interpolated climate surfaces for global land areas. *International Journal of Climatology*, *25*(15), 1965–1978. https://doi.org/10.1002/joc.1276

Holderegger, R., Buehler, D., Gugerli, F., & Manel, S. (2010). Landscape genetics of plants. *Trends in Plant Science*, *15*(12), 675–683. https://doi.org/10.1016/j.tplants.2010.09.002

Kharouba, H. M., Lewthwaite, J. M. M., Guralnick, R., Kerr, J. T., & Vellend, M. (2019). Using insect natural history collections to study global change impacts: Challenges and opportunities. *Philosophical Transactions of the Royal Society B: Biological Sciences*, *374*(1763), 20170405. https://doi.org/10.1098/rstb.2017.0405

Lee, C. R., & Mitchell-olds, T. (2011). Quantifying effects of environmental and geographical factors on patterns of genetic differentiation. *Molecular Ecology*, *20*(22), 4631–4642. https://doi.org/10.1111/j.1365-294X.2011.05310.x

Ma, X., Wang, Z., Tian, B., & Sun, H. (2019). Phylogeographic analyses of the East Asian endemic genus Prinsepia and the role of the East Asian monsoon system in shaping a North-South divergence pattern in China. *Frontiers in Genetics*, *10*, 128–128. https://doi.org/10.3389/fgene.2019.00128

Manel, S., Schwartz, M. K., Luikart, G., & Taberlet, P. (2003). Landscape genetics: Combining landscape ecology and population genetics. *Trends in Ecology & Evolution*, *18*(4), 189–197. https://doi.org/10.1016/S0169-5347(03)00008-9

Manthey, J. D., & Moyle, R. G. (2015). Isolation by environment in White-breasted Nuthatches (*Sitta carolinensis*) of the Madrean Archipelago sky islands: A landscape genomics approach. *Molecular Ecology*, *24*(14), 3628–3638.

McCauley, D. E. (1994). Contrasting the distribution of chloroplast DNA and allozyme polymorphism among local populations of Silene alba: Implications for studies of gene flow in plants. *Proceedings of the National Academy of Sciences of the United States of America*, *91*(17), 8127–8131. https://doi.org/10.1073/pnas.91.17.8127

McRae, B. H., Dickson, B. G., Keitt, T. H., & Shah, V. B. (2008). Using circuit theory to model connectivity in ecology, evolution, and conservation. *Ecology*, *89*(10), 2712–2724. https://doi.org/10.1890/07-1861.1

Meirmans, P. G. (2012). The trouble with isolation by distance. *Molecular Ecology*, *21*(12), 2839–2846. https://doi.org/10.1111/j.1365-294X.2012.05578.x

Milne, R. I., & Abbott, R. J. (2002). The origin and evolution of tertiary relict floras. *Advances in Botanical Research*, *38*, 281–314.

Oksanen, J., Blanchet, F. G., Kindt, R., Legendre, P., & Minchin, P. (2017). The vegan package: Community ecology package. R package version 2.4–2. Retrieved from https://CRAN.R-project.org/package=vegan

Palma-Silva, C., Lexer, C., Paggi, G. M., Barbará, T., Bered, F., & Bodanese-Zanettini, M. H. (2009). Range-wide patterns of nuclear and chloroplast DNA diversity in *Vriesea gigantea* (Bromeliaceae), a neotropical forest species. *Heredity*, *103*(6), 503–512. https://doi.org/10.1038/hdy.2009.116

Pauwels, M., Vekemans, X., Godé, C., Frérot, H., Castric, V., & Saumitou-Laprade, P. (2012). Nuclear and chloroplast DNA phylogeography reveals vicariance among European populations of the model species for the study of metal tolerance, *Arabidopsis halleri* (Brassicaceae). *New Phytologist*, *193*(4), 916–928. https://doi.org/10.1111/j.1469-8137.2011.04003.x

Peakall, R., & Smouse, P. E. (2012). GenAlEx 6.5: Genetic analysis in Excel. Population genetic software for teaching and research—An update. *Bioinformatics*, *28*(19), 2537–2539.

Pearson, R. G., & Dawson, T. P. (2003). Predicting the impacts of climate change on the distribution of species: Are bioclimate envelope models useful? *Global Ecology and Biogeography*, *12*(5), 361–371.

Pelletier, T. A., & Carstens, B. C. (2018). Geographical range size and latitude predict population genetic structure in a global survey. *Biology Letters*, *14*(1), 20170566. https://doi.org/10.1098/rsbl.2017.0566

Phillips, S. J., & Dudík, M. (2008). Modeling of species distributions with Maxent: New extensions and a comprehensive evaluation. *Ecography*, *31*(2), 161–175. https://doi.org/10.1111/j.0906-7590.2008.5203.x

Phillipsen, I. C., Kirk, E. H., Bogan, M. T., Mims, M. C., Olden, J. D., & Lytle, D. A. (2015). Dispersal ability and habitat requirements determine landscape-level genetic patterns in desert aquatic insects. *Molecular Ecology*, *24*(1), 54–69. https://doi.org/10.1111/mec.13003

Phillipsen, I. C., & Lytle, D. A. (2013). Aquatic insects in a sea of desert: Population genetic structure is shaped by limited dispersal in a naturally fragmented landscape. *Ecography*, *36*(6), 731–743. https://doi.org/10.1111/j.1600-0587.2012.00002.x

Qian, H., & Ricklefs, R. E. (2000). Large-scale processes and the Asian bias in species diversity of temperate plants. *Nature*, *407*(6801), 180–182. https://doi.org/10.1038/35025052

Qian, H., & Ricklefs, R. E. (2004). Geographical distribution and ecological conservatism of disjunct genera of vascular plants in eastern Asia and eastern North America. *Journal of Ecology*, *92*(2), 253–265. https://doi.org/10.1111/j.0022-0477.2004.00868.x

Qiu, Y. X., Fu, C. X., & Comes, H. P. (2011). Plant molecular phylogeography in China and adjacent regions: Tracing the genetic imprints of Quaternary climate and environmental change in the world's most diverse temperate flora. *Molecular Phylogenetics and Evolution*, *59*(1), 225–244. https://doi.org/10.1016/j.ympev.2011.01.012

R Development Core Team. (2013). *R: A language and environment for statistical computing*. Vienna, Austria: R foundation for Statistical Computing.

Rissler, L. J. (2016). Union of phylogeography and landscape genetics. *Proceedings of the National Academy of Sciences of the United States of America*, *113*(29), 8079–8086. https://doi.org/10.1073/pnas.1601073113

Rozas, J., Ferrer-Mata, A., Sanchez-DelBarrio, J. C., Guirao-Rico, S., Librado, P., Ramos-Onsins, S. E., & Sanchez-Gracia, A. (2017). DnaSP 6: DNA sequence polymorphism analysis of large data sets. *Molecular Biology and Evolution*, *34*(12), 3299–3302. https://doi.org/10.1093/molbev/msx248

Sakaguchi, S., Qiu, Y.-X., Liu, Y.-H., Qi, X.-S., Kim, S.-H., Han, J., ... Isagi, Y. (2012). Climate oscillation during the Quaternary associated

with landscape heterogeneity promoted allopatric lineage divergence of a temperate tree *Kalopanax septemlobus* (Araliaceae) in East Asia. *Molecular Ecology*, *21*(15), 3823–3838. https://doi.org/10.1111/j.1365-294x.2012.05652.x

Sexton, J. P., Hangartner, S. B., & Hoffmann, A. A. (2014). Genetic isolation by environment or distance: Which pattern of gene flow is most common? *Evolution*, *68*(1), 1–15.

Shafer, A. B. A., & Wolf, J. B. W. (2013). Widespread evidence for incipient ecological speciation: A meta-analysis of isolation-by-ecology. *Ecology Letters*, *16*(7), 940–950. https://doi.org/10.1111/ele.12120

Shah, V. B., & McRae, B. H., (2008). Circuitscape: A tool for landscape ecology. In G. Varoquaux, T. Vaught, & J. Millman (Eds.), *Proceedings of the 7th Python in Science Conference (SciPy 2008)* (pp. 62–66) Pasadena, CA.

Shields, C. A., Bailey, D. A., Danabasoglu, G., Jochum, M., Kiehl, J. T., Levis, S., & Park, S. (2012). The low-resolution CCSM4. *Journal of Climate*, *25*(12), 3993–4014. https://doi.org/10.1175/JCLI-D-11-00260.1

Smith, C. G., Hamel, P. B., Devall, M. S., & Nathan, M. S. (2004). Hermit thrush is the first observed dispersal agent for pondberry (*Lindera melissifolia*). *Castanea*, *69*(1), 1–8. https://doi.org/10.2179/0008-7475(2004)069<0001:HTITFO>2.0.CO;2

Soltis, D. E., Morris, A. B., McLachlan, J. S., Manos, P. S., & Soltis, P. S. (2006). Comparative phylogeography of unglaciated eastern North America. *Molecular Ecology*, *15*(14), 4261–4293. https://doi.org/10.1111/j.1365-294X.2006.03061.x

Tang, C. Q., Matsui, T., Ohashi, H., Dong, Y.-F., Momohara, A., Herrando-Moraira, S., ... López-Pujol, J. (2018). Identifying long-term stable refugia for relict plant species in East Asia. *Nature Communications*, *9*(1), 4488. https://doi.org/10.1038/s41467-018-06837-3

van Boheemen, L. A., Atwater, D. Z., & Hodgins, K. A. (2019). Rapid and repeated local adaptation to climate in an invasive plant. *New Phytologist*, *222*(1), 614–627. https://doi.org/10.1111/nph.15564

Van der Putten, W. H., Macel, M., & Visser, M. E. (2010). Predicting species distribution and abundance responses to climate change: Why it is essential to include biotic interactions across trophic levels. *Philosophical Transactions of the Royal Society of London. Series B, Biological Sciences*, *365*(1549), 2025–2034. https://doi.org/10.1098/rstb.2010.0037

Vasconcellos, M. M., Colli, G. R., Weber, J. N., Ortiz, E. M., Rodrigues, M. T., & Cannatella, D. C. (2019). Isolation by instability: Historical climate change shapes population structure and genomic divergence of treefrogs in the Neotropical Cerrado savanna. *Molecular Ecology*, *28*(7), 1748–1764. https://doi.org/10.1111/mec.15045

Wang, I. J. (2010). Recognizing the temporal distinctions between landscape genetics and phylogeography. *Molecular Ecology*, *19*(13), 2605–2608. https://doi.org/10.1111/j.1365-294X.2010.04715.x

Wang, I. J., & Bradburd, G. S. (2014). Isolation by environment. *Molecular Ecology*, *23*(23), 5649–5662. https://doi.org/10.1111/mec.12938

Wang, I. J., Glor, R. E., & Losos, J. B. (2013). Quantifying the roles of ecology and geography in spatial genetic divergence. *Ecology Letters*, *16*(2), 175–182. https://doi.org/10.1111/ele.12025

Wang, T., Zhu, Q., Heller, K. G., Zhou, Z., & Shi, F. (2020). Phylogenetic relationships and phylogeography of the genus *Sinocyrtaspis* Liu, 2000 (Orthoptera: Tettigoniidae: Meconematinae) reveal speciation processes related to climate change. *Systematic Entomology*, *45*(1), 144–159.

Watanabe, S., Hajima, T., Sudo, K., Nagashima, T., Takemura, T., Okajima, H., ... Kawamiya, M. (2011). MIROC-ESM 2010: Model description and basic results of CMIP5-20c3m experiments. *Geoscientific Model Development*, *4*(4), 845–872. https://doi.org/10.5194/gmd-4-845-2011

Wright, S. (1943). Isolation by distance. *Genetics*, *28*(2), 114–138.

Ye, J. W., Bai, W. N., Bao, L., Wang, T. M., Wang, H. F., & Ge, J. P. (2017). Sharp genetic discontinuity in the aridity-sensitive *Lindera obtusiloba* (Lauraceae): Solid evidence supporting the Tertiary floral subdivision

in East Asia. *Journal of Biogeography*, *44*(9), 2082–2095. https://doi.org/10.1111/jbi.13020

Zhang, Y. H., Wang, I. J., Comes, H. P., Peng, H., & Qiu, Y. X. (2016). Contributions of historical and contemporary geographic and environmental factors to phylogeographic structure in a Tertiary relict species, *Emmenopterys henryi* (Rubiaceae). *Scientific Reports*, *6*, 24041. https://doi.org/10.1038/srep24041

SUPPORTING INFORMATION

Additional supporting information may be found online in the Supporting Information section.